

Technical Note

Cross section reconcondensation method via generalized energy condensation theory

Steven Douglass, Farzad Rahnema*

Nuclear and Radiological Engineering/Medical Physics Programs, George W. Woodruff School, Georgia Institute of Technology, Atlanta, GA 30332-0405, United States

ARTICLE INFO

Article history:

Received 3 March 2011

Received in revised form 20 April 2011

Accepted 21 April 2011

Available online 31 May 2011

Keywords:

Neutron transport

Cross section

Recondensation

Multigroup theory

Core-environment effect

Energy

ABSTRACT

The standard multigroup method used in whole-core reactor analysis relies on energy condensed (coarse-group) cross sections generated from single lattice cell calculations, typically with specular reflective boundary conditions. Because these boundary conditions are an approximation and not representative of the core environment for that lattice, an error is introduced in the core solution (both eigenvalue and flux). As current and next generation reactors trend toward increasing assembly and core heterogeneity, this error becomes more significant. The method presented here corrects for this error by generating updated coarse-group cross sections on-the-fly within whole-core reactor calculations without resorting to additional cell calculations. In this paper, the fine-group core flux is unfolded by making use of the recently published Generalized Condensation Theory and the cross sections are recondensed at the whole-core level. By iteratively performing this recondensation, an improved core solution is found in which the core-environment has been fully taken into account. This recondensation method is both easy to implement and computationally very efficient because it requires precomputation and storage of only the energy integrals and fine-group cross sections. In this work, the theoretical basis and development of cross section recondensation is presented, and the method is verified with several sample problems.

Published by Elsevier Ltd.

1. Introduction

The most common treatment of the energy variable in reactor analysis is multigroup method, used ubiquitously in neutron transport and diffusion codes. Its extensive use is predicated on the fact that solving fixed source or eigenvalue problems in large complicated systems such as reactors requires a prohibitive amount of computational cost (in both memory requirements and time). A fully resolved discretization of the phase space for a whole-core problem results in millions of unknowns; therefore, it is common practice, for the sake of efficiency and practicality, to coarsen the discretization by dividing the problem into three layers of approximation.

The first layer of approximation is to condense the cross section data from a point-wise, continuous energy framework into a fine (100s or 1000s of groups) or ultra-fine-group (10,000s of groups) format using a pin-cell calculation (typically a 1D cylindrical calculation). These cross sections are then used in an assembly-level transport calculation to produce coarse-group (usually < 10 groups) cross sections that are spatially homogenized over either the pin-cell or the entire assembly, introducing a second layer of approximation. These are then used in a whole-core nodal diffu-

sion or transport calculation, which introduces an additional layer of approximation in its angular and spatial discretization. This coarsening procedure allows the whole core problem to be solved efficiently by reducing the core problem from millions of unknowns to thousands; however, it also introduces approximations which reduce the accuracy of the core calculation.

The cross section condensation process is designed to preserve the fine-group neutron reaction rates in the condensed solution by defining the coarse-group cross sections as a flux-weighted average over the coarse groups. In theory, this would allow the core problem, solved with the fine-group cross sections, to yield the same reaction rates and eigenvalue as the core solved with the coarse-group cross sections. However, because this method requires the exact fine-group flux in order to construct the coarse-group cross sections, and because this core-level fine-group flux is not known *a priori*, an approximate flux must be used. Generally, the fine-group flux solution at the lattice cell (assembly) level with specular reflective boundary conditions is used as the approximate weighting function to condense the cross sections. However, when the lattice is placed into the core, the effect of neighboring bundles may result in strong flux gradients across the boundary (due to control blades, varying burnup, peripheral effects, etc). In these cases, the specular-reflective boundary condition used in the lattice calculation is not a good approximation of the core environment, and results in coarse-group cross sections that do not preserve the fine-group reaction rates of the core problem.

* Corresponding author.

E-mail addresses: douglass.steven@gmail.com (S. Douglass), farzad@gatech.edu (F. Rahnema).

In this paper, a new method is presented which addresses this problem by taking advantage of the recent development of a Generalized Energy Condensation (GEC) Theory (Rahnama et al., 2008; also see Zhu and Forget, 2010), which allows an approximation of the fine-group flux at the core level to be unfolded during the coarse-group calculation. This flux is an approximation of the fine-group flux in the core, but because the cross section moments were condensed with the lattice cell flux, the previous papers were unable to improve the integral quantities of the core calculation (coarse-group flux, reaction rates, and eigenvalue).

The basis of the recondensation method presented here is to use the unfolded flux from GEC as a new weighting function to generate updated coarse-group cross sections on the fly during the core calculation, and re-solving the core problem with the updated cross sections. By iterating on this procedure, an improved approximation of the integral quantities of the core can be found which accounts for the effects of the core environment.

2. Background

2.1. Generalized energy condensation theory

The basis of the Generalized Energy Condensation theory is the expansion of the angular flux into a series of orthogonal functions ξ_n within each coarse energy group. This expansion is presented in Eq. (1), in terms of lethargy (scaled to the interval $u_- < u_g < u_+$) within coarse group g .

$$\begin{aligned}\Psi(\vec{r}, \hat{\Omega}, u_g) &= \sum_{n=0}^{\infty} \alpha_n \xi_n(u_g) \int_{u_-}^{u_+} du'_g \Psi(\vec{r}, \hat{\Omega}, u'_g) w(u'_g) \xi'_n(u_g) \\ &= \sum_{n=0}^{\infty} \alpha_n \xi_n(u_g) \Psi_n(\vec{r}, \hat{\Omega})\end{aligned}\quad (1)$$

whereas the standard condensation process (0th order of the GEC method), preserves only the integral reaction rates within each coarse group, when Eq. (1) is inserted into the transport equation, the fine-group flux spectrum of the assembly calculation is preserved by folding it into higher-order moments of the coarse-group cross sections, as in Eq. (2).

$$\sigma_{ng}(\vec{r}) = \frac{\int_{u_-}^{u_+} du'_g \sigma(\vec{r}, u'_g) \Phi(\vec{r}, \hat{\Omega}, u'_g) w(u'_g) \xi'_n(u_g)}{\int_{u_-}^{u_+} du'_g \Phi(\vec{r}, \hat{\Omega}, u'_g)} \quad (2)$$

This method has been demonstrated with Legendre polynomials, which have several advantages over other orthogonal functions. They are commonly used in the industry to approximate the angular dependence of the flux (spherical harmonics), the weighting function is equal to unity, and because all higher order moments integrate to zero, the expansion equations (Eq. (3)) become decoupled in order, which allows for very efficient solution of the higher order flux moments within the coarse-group core calculations.

$$\begin{aligned}\hat{\Omega} \cdot \nabla \Psi_{ng}(\vec{r}, \hat{\Omega}) + \sigma_{0g}(\vec{r}) \Psi_{ng}(\vec{r}, \hat{\Omega}) \\ = \sum_{g'=1}^G \left(\frac{\chi_{ng}(\vec{r})}{4\pi k} v \sigma_{fg'}(\vec{r}) \phi_{g'}(\vec{r}) + \sum_{l=0}^{\infty} \sum_{m=-l}^l Y_{lm}^*(\hat{\Omega}) \sigma_{sng' \rightarrow gl}(\vec{r}) \phi_{g'l}^m(\vec{r}) \right) \\ - \delta_{ng}(\vec{r}) \Psi_{0g}(\vec{r}, \hat{\Omega})\end{aligned}\quad (3)$$

where $Y_{lm}(\hat{\Omega})$ are the normalized spherical harmonics. Note that in Eq. (3) the total cross section has been separated into an energy independent term and an energy dependent term, as in Eq. (4), to eliminate the numerical instability in having higher order

expansion moments, which are often very small, in the denominator of the collision cross section moments.

$$\sigma(\vec{r}, u_g) = \sigma_{0g}(\vec{r}) + \delta(\vec{r}, u_g) \quad (4)$$

In addition, it is noted that Eq. (3) presents the expansion equations with the scattering expanded in Legendre Polynomials; however, the method is not restricted to any particular angular approximation of the scattering kernel. For a detailed derivation of the general expansion equations and examples of its implementation, see Rahnama et al. (2008). The GEC theory has been shown to be highly effective in extracting the fine-group energy dependence of the angular flux in a core calculation with little additional computational expense over the standard coarse-group method.

3. Method

Because the coarse-group cross sections are designed to preserve the fine-group reaction rates, an accurate condensed core calculation requires the exact fine-group flux in the core, which is unknown. As mentioned above, in the standard multigroup method, the lattice cell flux is used as an approximate weighting function; however, this introduces a significant source of error. The specular reflective boundary conditions of the lattice cell calculation are generally not an adequate approximation of the core environment, particularly in the heterogeneous configurations typical of current operating reactors. Because the lattice cell spectrum is not a good approximation, improving the coarse-group cross sections requires a different source of fine-group flux. By making use of the generalized condensation theory, a new core-level fine-group flux can be found which has been shown to be significantly closer to the fine-group core spectrum than it is to the lattice cell spectrum. As demonstrated by Rahnama et al. (2008), the expanded fine-group flux for a 1D BWR problem with a high order expansion (>10 energy moments) resulted in less than 3% average RMS error, in comparison with 15% RMS error for the lattice spectrum.

The basis of the recondensation method is therefore to treat the lattice spectrum merely as an initial guess for the weighting function, and to use the generalized energy condensation theory to generate a new approximation to core-level fine group flux by unfolding the coarse-group flux moments. The new spectrum, which is a better approximation for the core-level flux than the lattice cell spectrum, is then used to generate new cross section moments, and the method is repeated.

The recondensation method is described by the following procedure.

1. Perform a fine-group transport calculation at the lattice cell level and generate initial coarse group cross sections (and higher-order energy moments using generalized condensation) for each material, as in Eq. (5)

$$\sigma_{nG}^{(0)}(\vec{r}) = \frac{\sum_{g \in G} \sigma_g(\vec{r}) \frac{\Phi_g(\vec{r})}{(u_+ - u_-)} \int_{u_-}^{u_+} du'_g P_n(u'_g)}{\sum_{g \in G} \frac{\Phi_g(\vec{r})}{(u_+ - u_-)}} \quad (5)$$

where u_+ and u_- are the upper and lower lethargy bounds of fine group g within coarse group G , which is scaled to the interval of orthogonality of the expansion function $\xi_n(u_g)$. The “(0)” superscript indicates that these cross sections have undergone no recondensation iterations.

2. Use these coarse group cross section moments in a whole-core calculation with the generalized energy condensation theory to produce core-level flux moments. As a result of the Legendre decoupling associated with the generalized energy condensation theory, the core calculation is performed just as in the standard multigroup method, which is equivalent to the 0th

order expansion. Once the coarse-group 0th order flux moments are obtained, the higher moments of the flux are computed with Eq. (6). For simplicity, scattering has been assumed to be isotropic; however, this is not a general restriction of the method.

$$\begin{aligned} & \hat{\Omega} \cdot \nabla \Psi_{nG}^{(0)}(\vec{r}, \hat{\Omega}) + \sigma_{0G}(\vec{r}) \Psi_{nG}^{(0)}(\vec{r}, \hat{\Omega}) \\ &= \sum_{G'=1}^{G_{\max}} \frac{1}{4\pi} \left(\frac{\chi_{nG}(\vec{r})}{k} v \sigma_{fG'}(\vec{r}) \Phi_G^{(0)}(\vec{r}) + \Phi_G^{(0)} \sigma_{snG' \rightarrow G}(\vec{r}) \right) \\ & - \delta_{nG}(\vec{r}) \Psi_{0G}^{(0)}(\vec{r}, \hat{\Omega}) \end{aligned} \quad (6)$$

Just as in Eq. (5), the “(0)” superscript indicates that the flux has been generated with no reconcondensation iterations.

- Expand the core-level angular flux into the fine-group structure, as in Eq. (7)

$$\begin{aligned} \Psi_g^{(0)}(\vec{r}, \hat{\Omega}) &= \int_{u_-}^{u_+} du_g \sum_{n=0}^{\infty} \frac{2n+1}{2} \Psi_{nG}^{(0)}(\vec{r}, \hat{\Omega}) P_n(u_g) \\ &= \sum_{n=0}^{\infty} \frac{2n+1}{2} \Psi_{nG}^{(0)}(\vec{r}, \hat{\Omega}) \int_{u_-}^{u_+} du_g P_n(u_g) \end{aligned} \quad (7)$$

Of note is the fact that the integral of the Legendre polynomials of each fine group is independent of geometry or materials, and instead depends only on the fine and coarse-group structures, allowing for easy computation and storage of these integrals.

- Use this flux spectrum to generate an updated set of coarse-group cross section moments, as in Eq. (8).

$$\sigma_{nG}^{(1)}(\vec{r}) = \frac{\sum_{g \in G} \sigma_g(\vec{r}) \frac{\Phi_g^{(0)}(\vec{r})}{(u_+ - u_-)} \int_{u_-}^{u_+} du_g P_n(u_g)}{\sum_{g \in G} \frac{\Phi_g^{(0)}(\vec{r})}{(u_+ - u_-)}} \quad (8)$$

where the “(1)” indicates the cross sections are approximated with one reconcondensation. This spectral correction to the core cross sections serves as an improvement over the original calculation, allowing for a more accurate calculation of the core flux and eigenvalue.

- Repeat steps 2–4 until the flux convergence criterion of Eq. (9) is met.

$$\varepsilon_G(\vec{r}) = 100 \frac{\Phi_{0G}^{(i+1)}(\vec{r}) - \Phi_{0G}^{(i)}(\vec{r})}{\Phi_{0G}^{(i)}(\vec{r})} < \varepsilon = \text{constant} \quad \forall(\vec{r}, G) \quad (9)$$

This reconcondensation method leads to an improved flux solution at the whole-core level which does not contain the error inherent in the use of specular boundary conditions in the lattice cell calculation. This error is significantly amplified in heterogeneous cores, particularly near strong absorbers (e.g., control rods and burnable poisons) and at interfaces with large material discontinuities, including peripheral assemblies.

An interesting property of the reconcondensation method is that it uses the lattice cell calculation as only an initial guess for the iterative procedure. As in most iterative processes, while the speed of convergence is strongly affected by the use of a good initial guess, the final converged solution of the iterative process is independent, and will be the same for any initial guess. This makes the reconcondensation method essentially independent of the lattice cell calculation, and by iterating between the expanded spectrum and the coarse-group core calculations, the core solution could be obtained without performing the lattice calculation. As a result, the reconcondensation solution can be thought of as an intrinsic solution of the core, depending only on the cross section mesh, group structure, and order of expansion, rather than as a merely a correction to the lattice cell spectrum.

The implementation of the reconcondensation method results in the need to balance the optimization of the initial guess versus the data handling and storage requirements. While the lattice solution does generate a more rapid convergence, the computational

requirements (solution time and memory) of the lattice calculation may cause the solution of the lattice problem to be more expensive than the added iterations from a non-optimized initial guess. A detailed analysis of this optimization problem is case-specific, and therefore left to the reader for their particular implementation. For the results presented in the next section, the lattice cell flux is the initial guess.

4. Method verification

In order to provide a verification of the reconcondensation method, the method has been implemented within a 1D discrete ordinates framework. This reduction allows the problem to be simplified and easily implemented, but does not restrict the general utility of the method. Within this context, the GEC equation solved for the whole core problem reduces from Eqs. (6) to (10).

$$\begin{aligned} \mu \frac{\partial \Psi_{nG}^{(0)}(x, \mu)}{\partial x} + \sigma_{0G}(x) \Psi_{nG}^{(0)}(x, \mu) &= \sum_{G'=1}^{G_{\max}} \left(\frac{\chi_{nG}(x)}{2k} v \sigma_{fG'}(x) \Phi_{G'}^{(0)}(x) \right. \\ & \left. + \Phi_{G'}^{(0)} \sigma_{snG' \rightarrow G}(x) \right) - \delta_{nG}(x) \Psi_{0G}^{(0)}(x, \mu) \end{aligned} \quad (10)$$

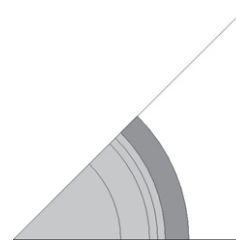
In order to test the reconcondensation method in a variety of situations, it is important to have a flexible set of benchmark problems of varying complexity. In order to accomplish this, a new set of 1D benchmark problems at both the lattice and core level has been developed here. The benchmark problems are composed of the different pin cells used in the GE9 BWR bundle (Kelly, 1995). The pin cell was modeled in the lattice cell depletion code HELIOS (Simeonov, 2003), with 1/8th symmetry and full specular reflection on all sides, as seen in Fig. 1. For each of several fuel enrichments, 47-group homogenized cross sections (flux-weighted) were generated for the entire pin cell from a 47-group transport calculation with the HELIOS 47-group unadjusted cross section library.

Twelve different fuel types (10 enrichments + 2 gadded) were used to generate cross sections, corresponding to the 12 fuel pin types used in the GE9 bundle. The number densities of the fuel materials are presented in Table 1. Fuels 11 and 12 contain Gd with the number densities labeled “Gd” in the Table. In order to add heterogeneity to the 1D problems, an additional cross section set was generated for the moderator region of the pin cell for fuel type 1.

These calculations result in 13 cross section sets (12 fuel types and 1 moderator) and allow the buildup of a variety of 1D benchmark problems. By varying the amount and location of Gd and moderator slabs, strong flux gradients representing the more challenging aspects of 2D and 3D core models can be simulated in a straightforward and flexible way.

4.1. 1D BWR single bundle

In order to provide a preliminary test of the method, a simplified 1D BWR bundle was constructed. The bundle is composed of 10 material regions (8 fuel-pin regions + moderator region on both sides). The fuel regions are each 1.6256 cm in width, and the



Cell Pitch	1.62560 cm
Fuel Radius	0.53213 cm
Incremental Fuel	0.37627 cm
Fuel Radii	0.47595 cm
	0.50482 cm
Clad Radius	0.61341 cm

Fig. 1. GE9 pin cell geometry.

Table 1Material composition for GE9 pin cell ($10^{24}/\text{cm}^2$).

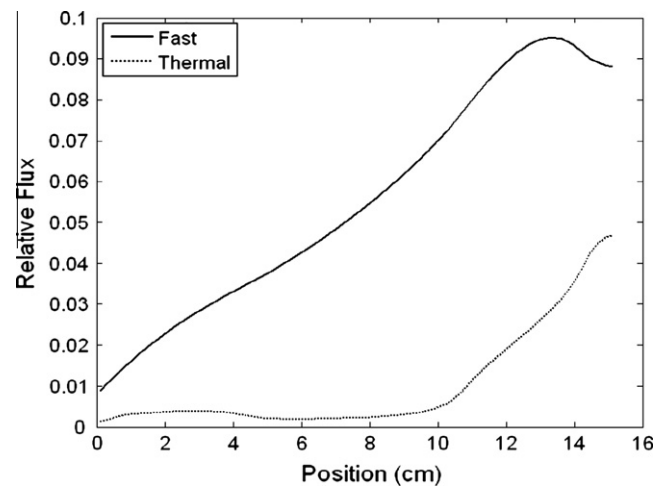
Fuel type	O	^{234}U	^{235}U	^{238}U		
1	4.4896E-2	3.1503E-6	3.6369E-4	4.4896E-2		
2	4.4898E-2	4.0177E-6	4.5461E-4	2.1991E-2		
3	4.4899E-2	4.4514E-6	5.0007E-4	2.1945E-2		
4	4.4900E-2	4.8851E-6	5.4553E-4	2.1900E-2		
5	4.4901E-2	5.3189E-6	5.9099E-4	2.1854E-2		
6	4.4902E-2	5.7526E-6	6.3645E-4	2.1809E-2		
7	4.4903E-2	6.1863E-6	6.8190E-4	2.1764E-2		
8	4.4907E-2	7.4874E-6	8.1828E-4	2.1628E-2		
9	4.4908E-2	7.9211E-6	8.6374E-4	2.1582E-2		
10	4.4908E-2	8.2406E-6	8.9783E-4	2.1548E-2		
11	4.4558E-2	7.8127E-6	8.5120E-4	2.0429E-2		
12	4.4556E-2	7.0985E-6	7.7578E-4	2.0504E-2		
	^{154}Gd	^{155}Gd	^{156}Gd	^{157}Gd	^{158}Gd	^{160}Gd
Gad	2.8746E-5	1.9550E-4	2.7045E-4	2.0677E-4	3.2819E-4	2.9121E-4
	H	O	Zr-Nat			
Mod	4.9316E-2	2.4658E-2				
Clad			4.3239E-2			

outside moderator regions are 1.1176 cm in width, accounting for 15.24 cm total bundle width (typical of BWR bundles). Both Gd and regular fuel regions are used in the bundle, laid out as in Fig. 2. Regions labeled “M” are moderator, and shaded regions are gadded fuel regions.

The bundle was modeled with full specular reflection on both boundary conditions and the 47-group spectrum was calculated with an S_8 approximation. This flux spectrum was used to condense the cross sections for each mesh into two groups, including the higher-order energy expansion moments from generalized condensation theory. These cross section moments were then used to solve the bundle again in two groups, but with one boundary condition changed to vacuum. This represents an extreme difference between the fine-group spectrum used to condense the cross sections and the actual fine-group solution to the problem. Fig. 3 presents the 2-group reference flux for the BWR bundle problem (left surface vacuum). The 2-group reference flux was obtained by energy-integrating the 47-group reference solution into the 2-group structure.

It was determined from previous work (Rahnama et al., 2008) that a 30th order expansion in energy is generally sufficient to represent the 47-group flux in each group using generalized energy condensation theory for BWR problems. The bulk of results here are therefore 30th order expansions. For the BWR bundle, the specular-reflective flux was used as the initial guess for the recondensation procedure, and the procedure was iterated until the maximum difference between the 2-group flux in successive iterations was less than $\varepsilon = 0.1\%$.

The eigenvalue results for the bundle are presented in Table 2. Three types of eigenvalue are presented in the table: k_{47} , k_{2ref} , k_{2rec} . The first, k_{47} , is the eigenvalue of the 47-group transport calculation. The second, k_{2ref} , is the eigenvalue of the 2-group calculation when the 47-group reference solution is used to generate the 2-group cross sections. This solution is the best condensed solution possible subject to the approximations of the condensation procedure, because the exact solution is used as the weighting function. The final eigenvalue, k_{2rec} , is the converged eigenvalue of the recondensation procedure. The final eigenvalue is presented for selected orders of expansion. The 0th order expansion represents the

**Fig. 3.** BWR bundle 2-group flux.**Table 2**

BWR bundle eigenvalue results.

	k_{47}	0.52680	
	k_{2ref}	0.55190	
	Order	k	δk^a
k_{2rec}	0	0.55903	713
	10	0.55638	448
	20	0.55282	92
	30	0.55279	89
	40	0.55266	76

^a δk is defined as $10^5 * (k_{2conv} - k_{2ref})$.

standard condensation method, using the specular reflective boundary condition flux to generate the cross sections.

The standard method (specular reflective boundary condition) results in an error of 713 pcm. The results indicate that as the expansion order increases, the recondensation method results in an improved eigenvalue, and for an expansion order greater than 20, the error reduces to less than 100 pcm. It is noted that while ~25 iterations were necessary to converge the flux to within $\varepsilon = 0.1\%$, most of the correction is accomplished within the first 5 or 6 iterations, and for the sake of practicality, could be stopped at that point for large problems.

**Fig. 2.** Single bundle layout including fuel material index.

As was mentioned in the previous section, a significant property of the recondensation method is the removal of dependence on the lattice cell calculation. This independence of the solution on the initial flux guess is demonstrated in Fig. 4.

In Fig. 4, the convergence of the recondensation eigenvalue is shown for two cases: (1) using the specular reflective boundary condition flux as the initial guess and (2) using a uniform and isotropic group flux ($\Psi_g^{(0)}(\vec{r}, \vec{\Omega}) = 1$) as the initial guess. The figure presents the eigenvalue of the 30th order recondensation method as a function of iteration. It is clear from the figure that the use of the specular boundary condition flux provided a significantly more rapid convergence than the use of the uniform flux, however the final solution is identical.

4.2. Full core problems

Because the bundle problem presented in the previous section is an extreme case, it is not representative of the actual neighbor-effects that the recondensation method is primarily intended to address. It is therefore desirable to construct core problems which are larger and more representative of the methods used in reactor analysis. In order to test the recondensation method in a larger framework, the homogenized cell cross sections produced from the GE9 pins were used to generate three 1D BWR Core Benchmark problems composed of four different 1D assembly types.

Each assembly is composed of 10 material regions (eight fuel-pin regions + moderator region on both sides). The fuel regions are each 1.6256 cm in width, and the outside moderator regions are 1.1176 cm in width, accounting for 15.24 cm total bundle width (typical of BWR bundles). Table 3 contains the layout of each bundle type by fuel type, with moderator regions shaded and labeled with an M and gadded pins striped. The bundle problems were modeled with specular reflective boundaries on both sides using a 1D discrete ordinates code (S_8), and the eigenvalue results (47-group S_8 calculation) are presented in the table.

The core geometries laid out as test problems for the recondensation method are composed of seven assemblies, with vacuum boundaries on both sides. Table 4 contains the core layout of three cores of increasing complexity, as well as the effective eigenvalue for each core, computed with a 47-group S_8 approximation.

Core 1 represents a relatively simple reactor problem, without sharp flux gradients due to the lack of highly absorbing regions and relative homogeneity. Core 2 includes 4 gadded fuel pins in 3 of the assemblies, introducing sharper thermal flux gradients and creating a more challenging problem for methods. Core 3 is a highly challenging configuration, as it includes three bundles made

Table 3
1D Bundle layouts.

Bundle #	Bundle layout										k_{inf}
1	M	3	3	8	8	8	8	3	3	M	1.32802
2	M	3	3	3	3	3	3	3	3	M	1.27464
3	M	3	3	11	11	11	11	3	3	M	0.73029
4	M	11	11	11	11	11	11	11	11	M	0.31612

Table 4
1D Core layouts by bundle type.

Core #	Core layout							k_{eff}
1	1	2	1	2	1	2	1	1.26528
2	1	3	1	3	1	3	1	1.03427
3	1	4	1	4	1	4	1	0.85857

up entirely of gadded pins, and contains very sharp thermal flux gradients at the boundary interfaces. The cores were modeled with $\frac{1}{2}$ symmetry (specular boundary condition on the right side, vacuum on the right), and the 2-group flux of each core, computed by integrating the 47-group solution over the standard 2-group range (thermal boundary 0.62506 eV), is presented in Fig. 5.

For each of the bundle types in the core, a transport solution was obtained with full specular reflection in an S_8 calculation, and the 47-group flux was used to generate 30th order coarse-group cross section moments using the GEC theory. This provided the initial guess cross sections for the recondensation method. As mentioned in the previous section, the recondensation solution is independent of the lattice cell flux, but is used as the initial guess here because it represents the standard approach in reactor analysis and allows for a more rapid convergence. These cross sections were then used to solve the core problems for the 30th order flux moments with coarse-group S_8 calculations. The expanded flux from the core calculation was used to iteratively condense the cross sections and re-perform the core calculation on the fly until the 2-group flux in successive iterations differed by a maximum of 0.1%. The eigenvalue results of the recondensation method are presented in Table 5. For each core, the 47-group reference eigenvalue (k_{47}), standard multigroup (no recondensation) eigenvalue (k_{2mg}), and the 30th order recondensation eigenvalue (k_{2rec}) are presented.

As seen in the table, the recondensation method with 30th order demonstrated an improvement in the eigenvalue over the

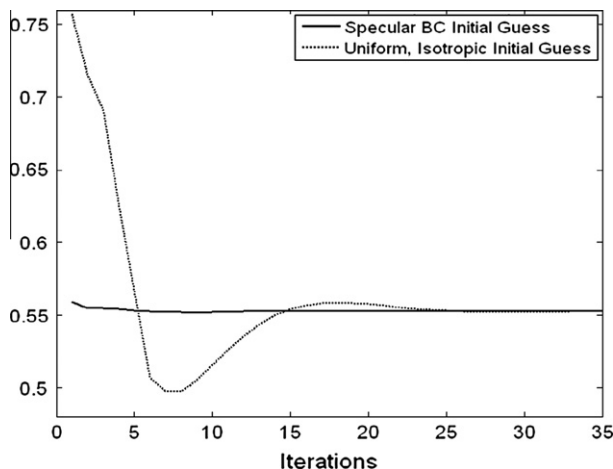


Fig. 4. Independence of initial guess in recondensation method.

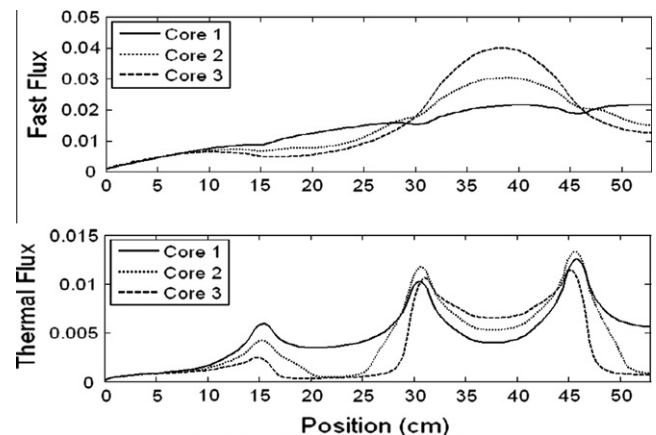


Fig. 5. 2-Group flux (47-group calculation) for benchmark cores.

Table 5
Core recondensation eigenvalue results.

	Order	Core 1		Core 2		Core 3	
k_{47}		1.26528	δk^a	1.03427	δk^a	0.85857	δk^a
k_{2ref}		1.27307		1.06028		0.90536	
k_{2rec}	0	1.27302	–5	1.07134	1106	0.93405	2869
	30	1.27193	–114	1.05214	–814	0.89052	–1484

^a δk is defined as $10^5 * (k_{2rec} - k_{2ref})$.

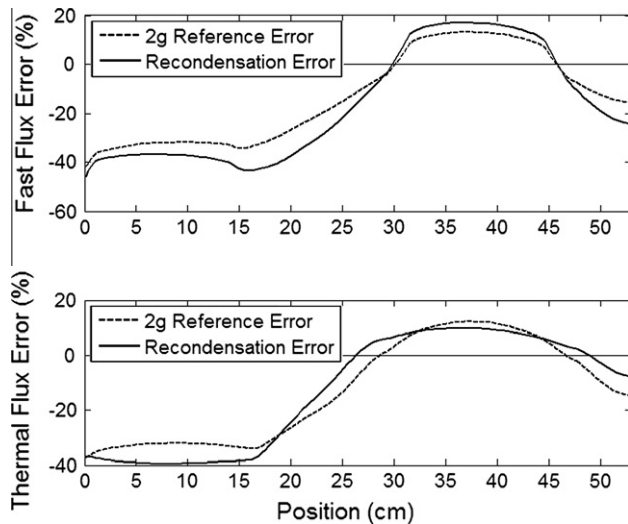


Fig. 6. Core 3 flux error (%) for 2-group reference solution and recondensation solution.

standard method (0th order) in Cores 2 and 3. In Core 1, the relatively more homogenous core results in a smoother flux behavior and lower bundle-to-bundle environment effects which reduces the utility of the recondensation scheme. In this case, the infinite-medium flux was able to provide a better solution as a result of error cancellation in the core calculation. In the more heterogeneous cores, where environmental effect is more pronounced, the recondensation method corrects for this effect.

Of interest from these results is that while the converged solution of the recondensation method accounts for the effects of the core environment, the eigenvalue does not exactly match the 47-group as one would expect. The large eigenvalue errors between the 2-group reference and the 47-group solution provide a likely explanation. Fig. 6 presents the %-difference in the 2-group flux between the solution obtained with the recondensation method and the direct 47-group solution as well as between the 2-group reference solution and the 47-group solution for Core 3. This core was chosen because it is the most heterogeneous and most challenging of the cores.

In both cases, as seen in Fig. 6, the errors are large and similar in magnitude. Further, the errors are significantly larger near the vacuum boundary, where the angular flux possesses a higher degree of anisotropy. In both methods, the angular dependence of the coarse-group total cross section is neglected, which is the source

of the error seen in the figure. This indicates that, while the recondensation method accounts for the core-environment effect, the energy-angle coupling still must be consistently accounted for in order to fully resolve the 47-group physics within the coarse-group calculation.

5. Summary and future work

A new method has been developed to correct for the effect of core environment in coarse-group core calculations. The industry standard method for whole-core reactor analysis relies on energy condensed (coarse-group) cross sections generated from single lattice cell calculations typically with specular reflective boundary conditions. Because these boundary conditions are an approximation and not representative of the core environment for that lattice, an error is introduced in the core solution (both eigenvalue and flux). The error becomes more significant with increasing assembly and core heterogeneity, a trend observed in current and next generation reactor designs.

The method presented here corrects for this error by generating updated coarse-group cross sections on-the-fly within whole-core reactor calculations. This is accomplished by making use of the GEC theory to unfold the fine-group core flux and recondense the cross sections at the whole-core level. By iteratively performing this recondensation, an improved core solution is found in which the core-environment effect has been fully taken into account. It is important to note that this theory requires precomputation and storage of only the energy integrals and fine-group cross sections. As a result, the recondensation method is both easy to implement and computationally very efficient.

It is also been demonstrated that the recondensation solution is an improvement over the standard multigroup method, and is particularly useful in core configurations that contain significant heterogeneity, which amplifies the core environment effect. As shown here, a significant factor in the accuracy of energy condensation methods is the treatment of the angular dependence of the coarse-group total cross section. The standard method typically neglects this dependence, or at best utilizes a first-order correction (e.g., consistent P_N approximation).

Although the recondensation method fully corrects for the core-environment, it is clear that for accurate calculations, one must simultaneously account for the effect of flux anisotropy on the collapsed total cross section. It is therefore desirable to develop a consistent generalized multigroup theory together with the recondensation method that accurately accounts for this energy-angle coupling in addition to the core environment effect.

References

- Rahnama, F., Douglass, S., Forget, B., 2008. Generalized energy condensation theory. *Nuclear Science and Engineering* 160 (1), 41–58.
- Simeonov, T., 2003. Release Notes – Helios System Version 1.8. Studsvik Scandpower Report, SSP-03/221, November 26.
- Kelly, D.J., 1995. Depletion of a BWR Lattice Using the RACER Continuous Energy Monte Carlo Code. In: *Proceedings of the International Conference on Mathematics and Computations, Reactor Physics, and Environmental Analyses*, vol. 2, Portland, Oregon, April 30–May 4, American Nuclear Society, p. 1011.
- Zhu, L., Forget, B., 2010. A discrete generalized multigroup energy expansion theory. *Nuclear Science and Engineering* 166 (3), 239–253.